



# Polymeric coating of surface modified nitinol stent with POSS-nanocomposite polymer

Raheleh Bakhshi<sup>a,b</sup>, Arnold Darbyshire<sup>a</sup>, James Eaton Evans<sup>c</sup>, Zhong You<sup>c</sup>, Jian Lu<sup>d</sup>, Alexander M. Seifalian<sup>a,e,\*</sup>

<sup>a</sup> University College London, Centre for Nanotechnology and Regenerative Medicine, London, UK

<sup>b</sup> Department of Mechanical Engineering, University College London, London, UK

<sup>c</sup> Department of Engineering Science, University of Oxford, Oxford, UK

<sup>d</sup> School of Physics and Astronomy, University of Manchester, Manchester, UK

<sup>e</sup> Royal Free Hampstead NHS Trust Hospital, London, UK

## ARTICLE INFO

### Article history:

Received 13 December 2010

Received in revised form 14 March 2011

Accepted 18 March 2011

Available online 4 April 2011

### Keywords:

NiTi

Nanocomposite

Surface modification

Aminosilane

Electrohydrodynamic spraying

Stent

## ABSTRACT

Stent angioplasty is a successful treatment for arterial occlusion, particularly in coronary artery disease. The clinical communities were enthusiastic about the use of drug-eluting stents; however, these stents have a tendency to be a contributory factor towards late stage thrombosis, leading to mortality in a significant number of patients per year.

This work presents an innovative approach in self-expanding coronary stents preparation. We developed a new nanocomposite polymer based on polyhedral oligomeric silsesquioxanes (POSS) and poly(carbonate-urea)urethane (PCU), which is an antithrombogenic and a non-biodegradable polymer with *in situ* endothelialization properties. The aim of this work is to coat a NiTi stent alloy with POSS-PCU. In prolonged applications in the human body, the corrosion of the NiTi alloy can result in the release of deleterious ions which leads to unwanted biological reactions. Coating the nitinol (NiTi) surface with POSS-PCU can enhance surface resistance and improve biocompatibility. Electrohydrodynamic spraying was used as the polymer deposition process and thus a few experiments were carried out to compare this process with casting. Prior to deposition the NiTi has been surface modified. The peel strength of the deposit was studied before and after degradation of the coating. It is shown that the surface modification enhances the peel strength by 300%. It is also indicated how the adhesion strength of the POSS-PCU coating changes post-exposure to physiological solutions comprised of hydrolytic, oxidative, peroxidative and biological media. This part of the study shows that the modified NiTi presents far greater resistance to decay in peel strength compared to the non-modified NiTi.

© 2011 Elsevier B.V. All rights reserved.

## 1. Introduction

Self-expanding stents have been introduced in intravascular stent technology in the past ten years for the treatment of peripheral disease. Drug eluting stent coatings to reduce restenosis rates is advancement. However, both these technologies have encountered difficulties. *In vivo* studies of the nitinol (NiTi) alloy material used in the construction of medical devices, including self-expanding stents, have shown that corrosion of the protective titanium (Ti) oxide layer can occur under certain conditions

resulting in the release of deleterious nickel (Ni) ions [1,2], which can provoke an inflammatory response and induce thrombus formation [3].

Drug eluting stent coatings were intended to improve the performance of bare metal stents by releasing an agent that inhibits neointimal hyperplasia [4]. Although the results of initial studies were encouraging and showed good patency rates, longer-term trials found the evidence of late-stage stent thrombosis compared with uncoated stents [5,6]. One reported hypothesis is that there is evidence that the eluted drug cause delayed re-endothelialization and normal cellular repair in and around the stent, which are important in preventing thrombosis and restenosis [7,8]. Evidence to support this can be found in results from preclinical animal studies which have shown that drug eluting stents can cause significant medial necrosis and persistent local fibrin deposition, suggesting delayed arterial healing compared with bare metal stents [9,10].

\* Corresponding author at: University College London, Centre for Nanotechnology and Regenerative Medicine, Royal Free Hampstead NHS Trust Hospital, Pond Street, London, UK. Tel.: +44 20 7830 2901.

E-mail address: [a.seifalian@ucl.ac.uk](mailto:a.seifalian@ucl.ac.uk) (A.M. Seifalian).

In addition, particle debris cracking off from porous, drug-eluting stents coatings can exaggerate inflammatory responses; counteract potential antiproliferative effects of drug delivery and, even worse, increase neointimal growth and luminal stenosis compared to bare stents [11].

Non-biodegradable polymer coatings may provide a solution for both of these problems as they can serve as a shield against corrosion and also as a platform for improving the biocompatibility of the device [12,13]. Polyurethanes are considered to be one of the most bio- and blood-compatible biomaterials known today and has been used in many biomedical application including development of intra-aortic balloons, catheters, pacemaker leads and medical tubings (Thermedics™ Polymer Products, Lubrizol Ltd.). Additional surface and/or bulk modification via attachments of biologically active species such as anticoagulants, cell proliferation suppressants are possible due to reactive groups, which are part of the polyurethane structure [14]. However, it is biodegradable for long term implantation and it lacks strength. Development of poly(carbonate-urea)urethane (PCU) increases the resistance to biodegradation in long term [15]. The small diameter graft made from this polymer has been used clinically as short term vascular access graft [16]. To enhance the anti-thrombogenicity of the PCU, we added polyhedral oligomeric silsesquioxanes (POSS) to the PCU structure and patented a non-biodegradable nanocomposite polymer based on POSS and PCU, where the POSS nanocages are pendant groups covalently attached to the polymer backbone (POSS–PCU). We have done large amount of tests on the polymer for biocompatibility *in vitro* and *in vivo*. This polymer is viscoelastic, durable, and has been shown to be biologically stable [17]. In addition, the POSS nanocages alter the surface morphology of the material, resulting in a surface that is non-thrombogenic [18]. Human endothelial progenitor cells adhere and proliferate on POSS–PCU [19], with the aim of *in situ* endothelialization [20,21]. Clinical trials of a small diameter bypass graft made from POSS–PCU are currently being conducted. This innovative polymer has been awarded top prizes in the field of cardiovascular in 2007 by medical future. In this work we have used this POSS–PCU to coat the NiTi stent. We have previously developed and optimised an electrohydrodynamic atomization (EHDA) deposition process for stent coating [22]. We have chosen this technique since the coating thickness can be precisely controlled [23].

A non-biodegradable coating must be able to withstand high strains during stent crimping and deployment without delamination or fracture and maintain its integrity for extended periods *in vivo* [24], otherwise it leads to several negative clinical complications. Damage to a coating may increase the risk of thrombosis [25]. The breakdown of the coating barrier causes the release of irritant or toxic ions from the metallic stent, leading to an inflammatory response. Debris from the coating caught in the blood stream could also create micro-embolisms [26,11]. The bond strength of the coating is highly dependent on the substrate surface condition [27] and a variety of treatments can be used to modify the surface and augment the bond strength. One standard approach is to increase the area available for bonding by increasing the surface roughness, but it does not provide the desired efficiency in long time. Because of the geometry of the stents, this technique is not applicable for the stents. Thus combining this method with other chemical or electrochemical surface modifications can result in coatings with durable bond strengths.

The Federal Drug Administration has recently provided guidance to the stent industry to evaluate the safeness and effectiveness of coated and drug-eluting stents [28]. Adhesion, barrier effectiveness, long-term stability and durability of the coating are a few of the requirements that need to be assessed to investigate the efficiency of the coating. Several examples in the literature report coating failures such as cracks and delamination especially

after stent expansion [29,30]. Delamination of polymer coatings on commercial stents [31] and coating damage *in vivo* has also been reported [32,33].

This paper describes surface modification to promote bond strength between the POSS–PCU nanocomposite and the surface of NiTi strips. The aim is to develop protocols with the potential for effective bonding of the polymer to NiTi in the development of small diameter stents; including coronary or peripheral stents. In this work the stability and the integrity of the POSS–PCU coating in pseudo-physiological solutions is also evaluated to determine whether the surface modification applied retains its effectiveness long-term.

## 2. Materials and methods

### 2.1. Synthesis of POSS–PCU polymer

The synthesis of the POSS–PCU nanocomposite (trade name; UCL-Nano™) has been described in detail previously [32]. Briefly, the inorganic urethane is made by dissolving silsesquioxane in poly(hexamethylene carbonate)diol, 4,4'-methylenebis (phenyl isocyanate) (MDI) was then added to polyol to produce pre-polymer. The pre-polymer blend was then chain extended with ethylene diamine in N,N'-dimethylacetamide (DMAC).

### 2.2. Surface modification

All chemicals used in this study were purchased from Sigma–Aldrich Limited, Gillingham, UK, unless stated otherwise. The nearly equiatomic NiTi alloy (55.8 wt.% Ni) strips used in this study were provided by Memry Corp., Bethel, USA. Rectangular samples (50 mm × 5 mm) were cut from 0.5 mm thick strips of the material. An oxide layer already exists on the alloy surface as a result of the manufacturing process. Sand blasting at a working distance of 200 mm was used to remove most of the existing oxide layer. Electrochemical anodisation was used in the next step to control and produce an oxide layer on the surface. Surface modification can be categorized in three different steps namely; electrochemical oxidation, heat treatment and silanisation.

A new electrochemical method, based on the work of Cheng et al. [33], was used to produce a titanium oxide (TiO<sub>2</sub>) coating on NiTi that involved anodising the Ti alloy in a methanolic electrolyte. The NiTi sample was immersed in an electrolyte prepared by dissolving 10 g of NaNO<sub>3</sub> (99.9%) in 1 litre of methanol. The sample was then galvanostatically anodised at the ambient temperature (20 °C) using a current density of  $3 \times 10^{-2}$  mA/mm<sup>2</sup> for 3 h with a pair of graphite rods as the cathode. The distance between anode NiTi and cathode was set at 20 mm for the anodisation process. The anodised samples were then left in the oven for 1 h at 600 °C. We called this step heat treatment.

3-Aminopropyltriethoxysilane ( $\gamma$ -APS) was applied to the surface as the coupling agent to chemically improve the adhesion between NiTi substrate and POSS–PCU film. It has three ethoxy groups and an amine group as an organofunctional group bound via a propyl group (–CH<sub>2</sub>–CH<sub>2</sub>–CH<sub>2</sub>–) link to the silicon atom. Prior to immersing in the silane solution, the anodised NiTi samples were cleaned by ultrasonic vibration (Kerry Ultrasonic Machine, North Yorkshire, UK) for 5 min in ethanol and then in acetone. The cleaned metals were then immersed in sodium hydroxide (NaOH) alkaline cleaner at 60 °C for 15 min to make sure there were sufficient OH groups to react with alkoxy functional groups, then rinsed with distilled water and dried in air. Solutions of 2 and 5 vol%  $\gamma$ -APS were prepared by diluting with ethanol/deionized water (95/5 vol%). The natural pH of the  $\gamma$ -APS solution was ~8 and the reaction can be catalysed with H<sup>+</sup> or OH<sup>–</sup>. Acetic acid was used to adjust it to

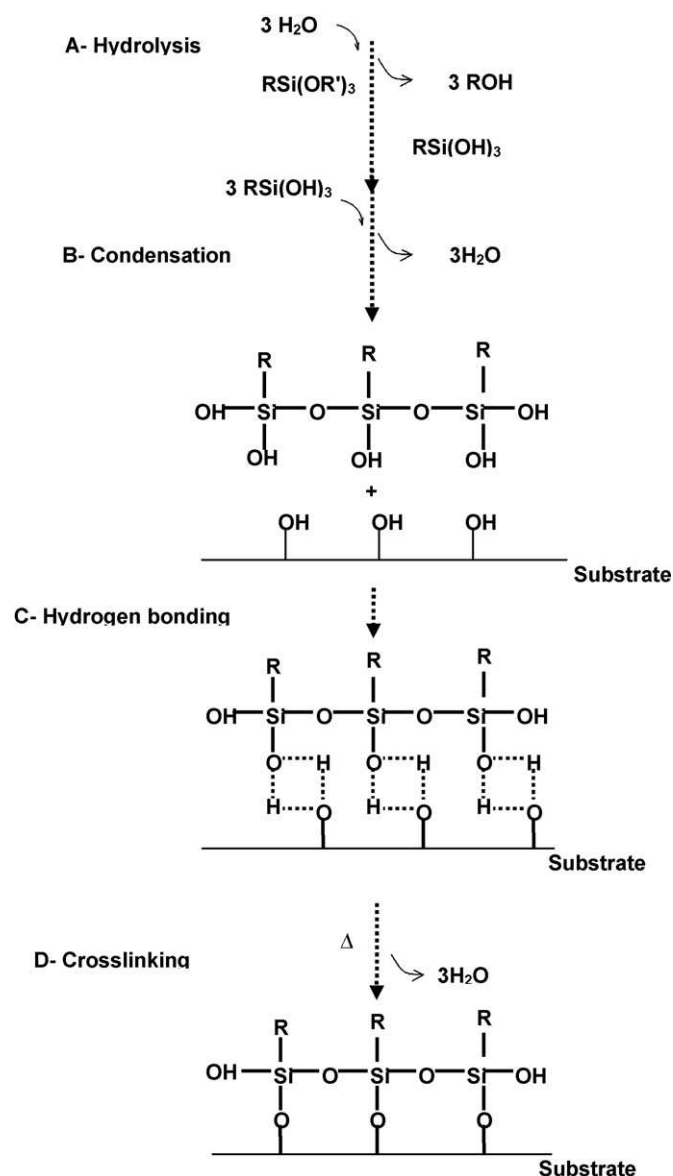


**Fig. 1.** Reaction stages of organotrialkoxysilane. (A) Hydrolysis, (B) condensation, (C) hydrogen bonding, and (D) crosslinking.

pH~4. These solutions were then activated and hydrolysed either for 15 min or for 60 min at the ambient temperature (23 °C). Concentration, pH and hydrolysis time are believed to have a significant effect on the effectiveness of the modification process [34].

The samples were then dipped into the freshly prepared silane solution, allowed to dry in air for 15 min and then cured at 110 °C for 20 min to crosslink the silane films. Thermal curing is well known to increase the crosslinking of silanes to form siloxane film on the NiTi surface. With the formation of chemical bonds between silane molecules and NiTi substrate, Si–O–Ti bonds are formed. The silanisation mechanism is illustrated in Fig. 1. The silanised strips were then primed with pre-polymer. Finally, the silanised NiTi strips were coated with polymer and placed in an oven overnight at 60 °C to remove any solvent.

### 2.3. Surface characterization

The morphology of the interface and the thickness of the surface layer formed on the NiTi samples were determined by scanning electron microscopy (SEM) using sample size of 10 mm. SEM was

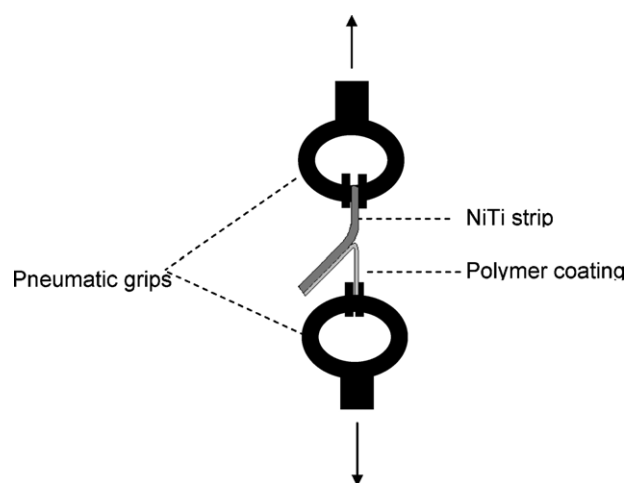


**Fig. 2.** Peel test arrangement. Arrows show the moving directions of the grips.

carried out using a JEOL JSM63101F scanning electron microscope equipped with an Energy Dispersive X-ray (EDX) analysis system. Prior to microscopy, samples were placed on aluminium stubs and the surface of interest was gold coated using an Edwards 5150B sputter coater. The accelerating voltage for SEM was 10 kV. The chemical composition of the coating was obtained using EDX analysis. Topographic analysis of the modified NiTi surface was carried out by a scanning probe microscope operated in atomic force microscopy (AFM) contact mode. The samples were analyzed by X-ray photoelectron spectroscopy (XPS) on a VG Scientific ESCALAB 5 spectrometer with monochromatic Al K $\alpha$  (120 W) X-ray radiation. The base pressure in the analysis chamber was better than 10<sup>−8</sup> mbar. Survey spectra acquired at 160 eV. High resolution scans were acquired at 40 eV pass energy to determine the chemical states and concentrations. The XPS depth profiles were obtained by using a rastered (2 mm<sup>2</sup>) 4 keV Argon ions beam. The system boasts a Quartz Catalytic Cell capable of pressures up to 6 bar at 400 °C or 1 bar at 1000 °C.

### 2.4. Coating of NiTi with POSS–PCU

In this study a sample of the 15 wt.% POSS–PCU solution was subjected to EHDA at 5.8 kV and 4  $\mu$ l/min in the stable cone-jet mode. Full details of the process have been given previously [30]. To complete the process of coating, the NiTi strip has to be sprayed for up to 3 h at room temperature. For comparison, POSS–PCU has been coated onto the NiTi using casting technique. The samples were kept in the oven held at 60 °C to evaporate the solvent.

### 2.5. Assessment of bond strength

An Instron 5565 tensometer equipped with a 500 N load cell was used to measure the peel strength of the POSS–PCU coated NiTi strips. The coated specimens were loaded in the test machine as shown in Fig. 2. Our approach is based on the ASTM D413 standard, which is used to determine the force per unit width required to separate a rubber layer from a flexible substrate such as fabric, fibre, wire, or sheet metal [35]. The standard detail methods for peeling the strip with the unpeeled portion held to give  $\alpha^\circ$  separation with moving grips. The adhesion strength is equal to the mean force recorded during the test. The peeling process was initiated manually. The lower machine grip was used to clamp the NiTi strip and the upper grip held the polymer film, with an initial distance of 10 mm between the grips. The test was conducted with a crosshead displacement rate of 5 mm/min to a final extension of 40 mm. Tests were conducted on specimens subjected to the

surface modification and on an unmodified strip, which acted as a control. Both electrosprayed and casted samples used for testing. For each type of modification, experimentation was done in triplicate. The thickness of the POSS–PCU coating on the samples tested was determined using SEM.

## 2.6. Stability of the coating

The susceptibility of POSS–PCU coated-NiTi to instability was assessed *in vitro* by incubating the coated strips of both modified and non-modified in biological/chemical solutions described below. These accelerated *in vitro* tests have shown good correlation with human and animal model results. The protocols have been modified in order to allow a repeatable and reproducible regime.

### 2.6.1. Hydrolysis with lysosomal enzymes

A solution of cholesterol esterase (CE) was prepared by dissolution of CE powder in a sterile, pH 7.0, 0.05 M phosphate buffered solution (PBS) at a concentration of 1 U mL<sup>-1</sup>. The standard 1 U is its ability to hydrolyse 1 mM min<sup>-1</sup> phosphatidylcholine at pH 8.0 at 37 °C. The other hydrolytic solution is phospholipase A2 solution (porcine pancreatic phospholipase, PLA), which was prepared in buffer solutions (50 mM Tris, pH 8.0, containing 6.8 mM CaCl<sub>2</sub>) at a concentration of 0.18 U mL<sup>-1</sup>.

### 2.6.2. Plasma protein fractions

Citrated human plasma (200 mL) derived from fresh frozen human plasma obtained from the Blood Transfusion Department at Royal Free Hospital, London, UK was placed in a beaker in a cold room (4 °C). Polyethyleneglycol (PEG, Mw = 3350) was added slowly, while stirring, to the plasma in the amount 10 g/100 mL. After 60 min of stirring, the 10% PEG precipitate, designated fraction I, was removed by centrifugation at 2000 rpm for 30 min. An additional 10 g of PEG was then added to the supernatant to reconstitute a 10% mixture followed by centrifugation to obtain fraction II (10–20% PEG precipitate). The process of mixing and centrifugation was then repeated to obtain four plasma protein fractions with the corresponding plasma fractions. The precipitates were reconstituted to the original volume of plasma (200 mL) with phosphate-buffered saline (Table 1).

### 2.6.3. Oxidation and peroxidation

The oxidative effect on the peel strength was also assessed using an oxygen donating system made by mixing 1.63 M of hydrogen peroxide (H<sub>2</sub>O<sub>2</sub>) and 0.1 M CoCl<sub>2</sub> 6 H<sub>2</sub>O (H<sub>2</sub>O<sub>2</sub>/CoCl<sub>2</sub>). The peroxidative system was prepared by combining 1.63 M *t*-butyl peroxide and 0.1 M CoCl<sub>2</sub> 6 H<sub>2</sub>O (*t*-but/CoCl<sub>2</sub>).

### 2.6.4. Control

Both modified and non-modified NiTi was incubated in distilled water under the same conditions to act as a negative control [15].

All the degradative solutions contained 10 mg streptomycin, 10,000 U penicillin per millilitre to prevent bacterial and fungal infections, which could affect the outcome of the results. Five coated NiTi strips were incubated in each solution (hydrolytic, oxidative, and plasma fractions) at 37 °C for 70 days on a shaker platform, and solutions were replaced weekly. After completion of the experiments, the samples were rinsed in distilled water, dried in air prior to microscopy and peel strength assessment.

## 2.7. Inductively coupled plasma mass spectrometry

Rectangular (30 mm × 5 mm) samples were cut from 0.5 mm thick NiTi strips. The surface modified NiTi strips were then primed with pre-polymer and finally coated with polymer. Dulbecco's modified Eagles' medium (DMEM) was used as the release medium

to further express the Ni release characteristics of NiTi. The samples were then incubated at 37 °C in 15 mL conical centrifuge tubes were filled with 5 mL of DMAC. One NiTi sample from each group removed at 1, 24, 48 and 72 h. The centrifuge tubes containing DMEM were then sent to the Mass Spectrometry Facility, King's College London for Inductively Coupled Plasma Mass Spectroscopy (ICP-MS) using a PerkinElmer Elan DRC+ with an AS93 autosampler. Data were managed using the PerkinElmer Elan v3.2 software. The experiments repeated three times and results averaged. The Ni release from these samples is compared to the Ni release from unmodified NiTi strip and bare NiTi as the control.

## 3. Results and discussion

### 3.1. Surface modification of NiTi

Chemical treatment induces a chemical bond between the polymer and the substrate. This approach requires a metal substrate which has an oxide layer that can enhance the polymer coating bond strength [27]. This oxide layer has been achieved using a variety of chemical, thermal and electrochemical pre-treatment methods [36]. Electrochemical reactions used in this study; which have been successfully used for degreasing, etching and oxidising metal surfaces, where the metal acts as an anode. The production of a protective Ti-rich oxide layer on the surface of superelastic NiTi alloys used in medical applications also improves the corrosion resistance of the material in physiological conditions [36]. The formation of TiO<sub>2</sub> provides the biocompatibility for this material by preventing release of Ni from the alloy into the body and because of the well known benign interactions of TiO<sub>2</sub> with the human body [37]. In some studies, oxide layers with a thickness of 50–300 nm have led to significant improvement in bond durability in an aqueous environment.

Primers may also be applied to substrate surfaces, and serve as coupling compounds to form a covalent bond with the metal and the polymer; such as silane (trialkoxysilanes) coupling agent [38]. In one patent [39], silane coupling agents are used to enhance the bonding of polymeric materials to metal substrates. The method involves depositing an oxide layer onto a metal followed by applying a silane coupling agent which forms a strong chemical bond with the oxide layer. This layer is then coated with a polymer. The silane promotes adhesion and protects the metal substrate by forming covalent bonds across the interface that are both strong and durable [40]. In silane surface treatment of metals, silane solutions can be applied onto surfaces by dipping and spraying [38].

Aminosilane bonds to the oxide layer and also provides a reactive amine group for subsequent reaction of isocyanate prepolymer coat. The hydrophobic siloxane layer is usually ten molecular layers thick (up to 800 nm), depending on the silane concentration [41]. The amine end of the silane molecule can polymerize with the isocyanate group of the POSS–PCU to form a urea group. The primer layer bridges between the medical implant and the drug-eluting matrix and provides optimal interactions with the surface of the implant and the outer layer and significantly improved the stability.

Therefore, the coating method has three steps where the anodisation process involves the formation of an oxide layer followed by heat treatment which then reacts with aminosilane. The schematic illustration of these bonding mechanisms between the reagents and NiTi strips is shown in Fig. 3.

### 3.2. Surface properties of NiTi after modification

At the end of the anodisation process, the sample surface appeared dark brown and was free of cracks, which is an indica-



**Table 1**  
Distribution of selected plasma proteins in the PEG fraction [48].

Plasma Proteins	Fraction wt.%(mg/dL)				Amount (mg/dL)
	I	II	III	IV	
Albumin	6 (206)	4 (138)	86 (2958)	100	3440
IgG	88 (651)	15 (111)	1 (7)	1	740
Transferrin	6 (13)	22 (49)	58 (129)	99	223
$\alpha$ 2-Macroglobulin	35 (66)	65 (123)	—	—	189
Fibrinogen	88 (158)	—	—	—	179
Ig(+)	34 (53)	58 (91)	20 (31)	—	157
Haptoglobin	2 (2)	40 (43)	56 (61)	86	108
$\alpha$ -Lipoprotein	15 (10)	25 (16)	50 (32)	50	64
C-3 component	93 (52)	7 (4)	—	—	56
$\alpha$ 1-Acid glycoprotein	—	—	100 $\pm$ 54	—	54
Ceruloplasmin	14 (3)	23 (5)	73 (16)	100	22
Plasminogen	69 (11)	19 (3)	—	89	16
$\beta$ -Lipoprotein	100 (16)	—	—	—	16
Prothrombin	25 (2)	50 (4)	25 (2)	—	8
C-1 esterase inhibitor	—	—	100 (4)	100	4

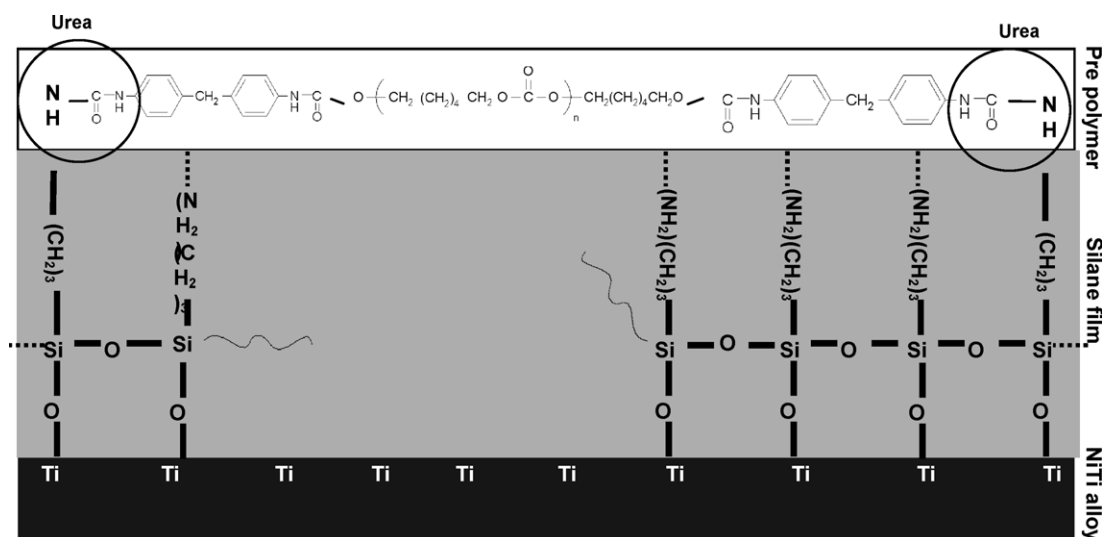


**Fig. 3.** Schematic illustration of the bonding mechanism between activated silane solution and NiTi.

tion of oxygen deficiency. Fig. 4 shows the cross-sectional views of the NiTi strips before and after anodisation. After anodisation, the thickness of the strip increased by 20  $\mu\text{m}$  and this indicates the formation of a uniform oxide layer (Fig. 4B). The measurement of the thickness of this layer was estimated up to the curvature which leads to the base of the metallic strips. These measurements compares well with 17  $\mu\text{m}$  reported by Cheng et al. [33]

who used a similar process and deposition time. However, these values are coarse when compared with other methods of preparing oxide layers on NiTi alloys. For example, oxide layers with a thickness of  $\sim 0.5 \mu\text{m}$  have been prepared using solution-based oxidation with hydrogen peroxide [42]. Furthermore, much finer oxide coatings (2 nm) can be prepared by controlling the partial pressure of oxygen in a selective oxidation process, but this requires

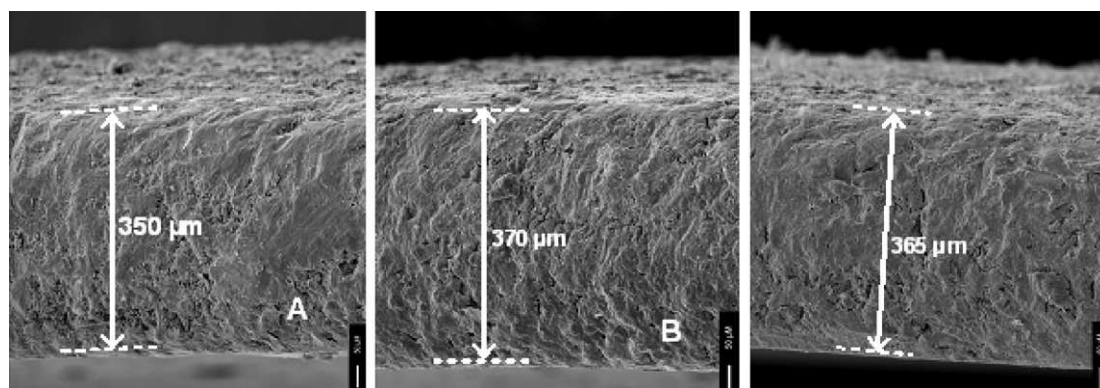


**Fig. 4.** Scanning electron micrographs showing the cross-sections of oxide coating on NiTi: (A) before anodisation, (B) after anodisation followed by (C) heat treatment at 600  $^{\circ}\text{C}$  for 1 h. Arrows show oxide layer.

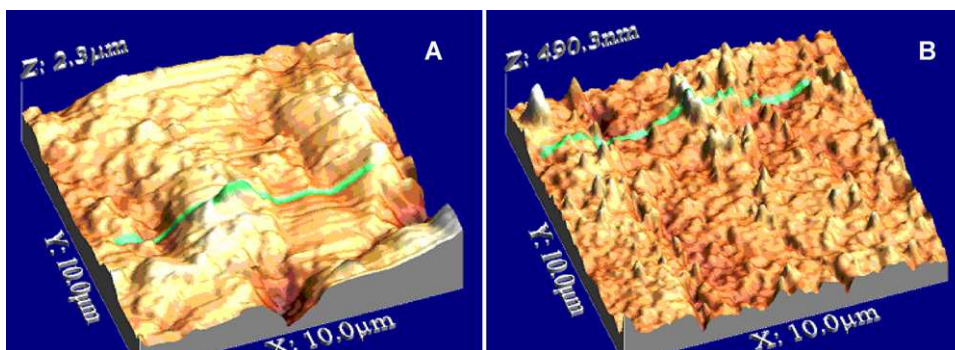


**Fig. 5.** Topography of anodised NiTi samples: (A) before heat treatment, and (B) after heat treatment at 600 °C.

more sophisticated equipment including the use of atmospheric sensors [43].

A current density of  $3 \times 10^{-2}$  mA/mm<sup>2</sup> was selected for the anodisation process. This value was selected based on previous studies [33], although the thickness of the NiTi strips in our application is much thicker (2 mm compared to 0.5 mm). With the anodisation process lasting for 3 h, it was anticipated that during this procedure the anode potential rises with time and can reach a value of 1.15 V, and these measurements have been used as indicators of coating thickness. The oxide layer thickness can be controlled by adjusting applied voltage and time to obtain thinner coatings for stents applications. It is postulated that TiO<sub>2</sub> is formed as a result of hydrolysis and polycondensation of titanium methoxide in the presence of water. Even if the surface layer is nickel oxide, it still provides a suitable platform for binding of aminosilane, since an oxide layer is required for silanisation. Electrolytic methods have been used to coat surfaces of NiTi alloys. For example thin tantalum coatings on NiTi alloys enhanced resistance to corrosion when placed in a 3.5% NaCl solution [44].

Fig. 4C shows the thickness of the modified NiTi strip was reduced by  $\sim 5$  µm after heat treatment at 600 °C for 1 h; compared with the thickness before heating. Hence on heating, densification occurs and the thickness of the coating is reduced.

The structure of these coatings (Fig. 4) shows the existence of micro to nanoscaled pores within the coating layer. Some pores are still evident in the post-heated coating, which means that an optimal heating temperature or time is desired. The aging of the oxide layers by heat treatment is also believed to reduce the ion dissolution and improve its alloy biocompatibility, which makes the material ideal for its application [45]. However, it should be noted that the mechanical response of the material is affected by heat treatment. A study of this effect has been carried out previously [46]. It showed that the material's austenite phase formation end temperature, which is critical to superelastic response, increases after heat treatment and is a function of heat treatment time and temperature. Careful management of the heat treatment process can be used to optimise the mechanical response of the material for the requirements of an intravascular device. Simply by changing temperature and duration of the heat treatment, one can optimise the procedure to maintain superelastic properties of the NiTi [46].

The surface morphology varies drastically between anodised and anodised-heat modified strips (Fig. 5). Anodised samples present micro-scaled topographical variations of the surface, which consist of valley and mountain like features. Upon thermal oxidation, which reinforces the initial oxidation process from the anodisation procedure, smaller sized nano-scaled peaks develop which make the surface more even. This is largely due to coalescence of the oxide layer, which results in a more homogenous surface. The oxygen (O) peak in the spectrum obtained for anodised NiTi confirms the presence of an oxide layer through anodisation

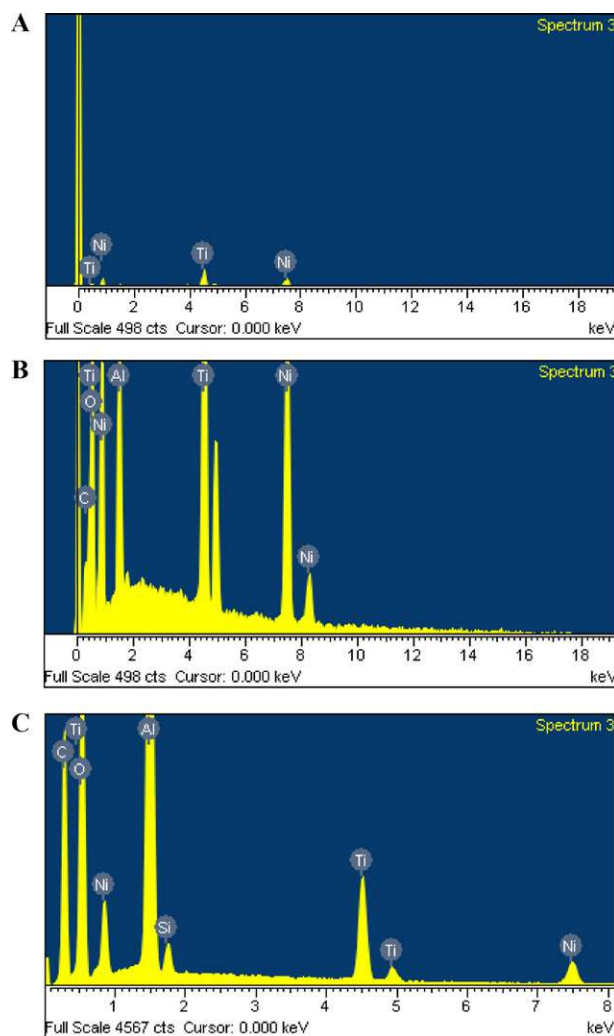


**Fig. 6.** Energy dispersive X-ray spectra of the modified NiTi. (A) As supplied before treatment, (B) after anodisation and (C) after silanisation.

(Fig. 6B). The O peak observed has the same order of intensity as the titanium peak; the major alloying element of NiTi. The intensity of the Ni peak is less than that of the Ti peak, which favours biocompatibility since it reduces the risk of nickel release.

The chemical composition of the NiTi surface after different silane modification conditions is compared in Table 2. The strip under modification (A) is rich in Si uniformly in all regions, whereas hardly any Si could be detected on all the regions selected for the rest of the surface by SEM/EDX. EDX analysis on the whole surface

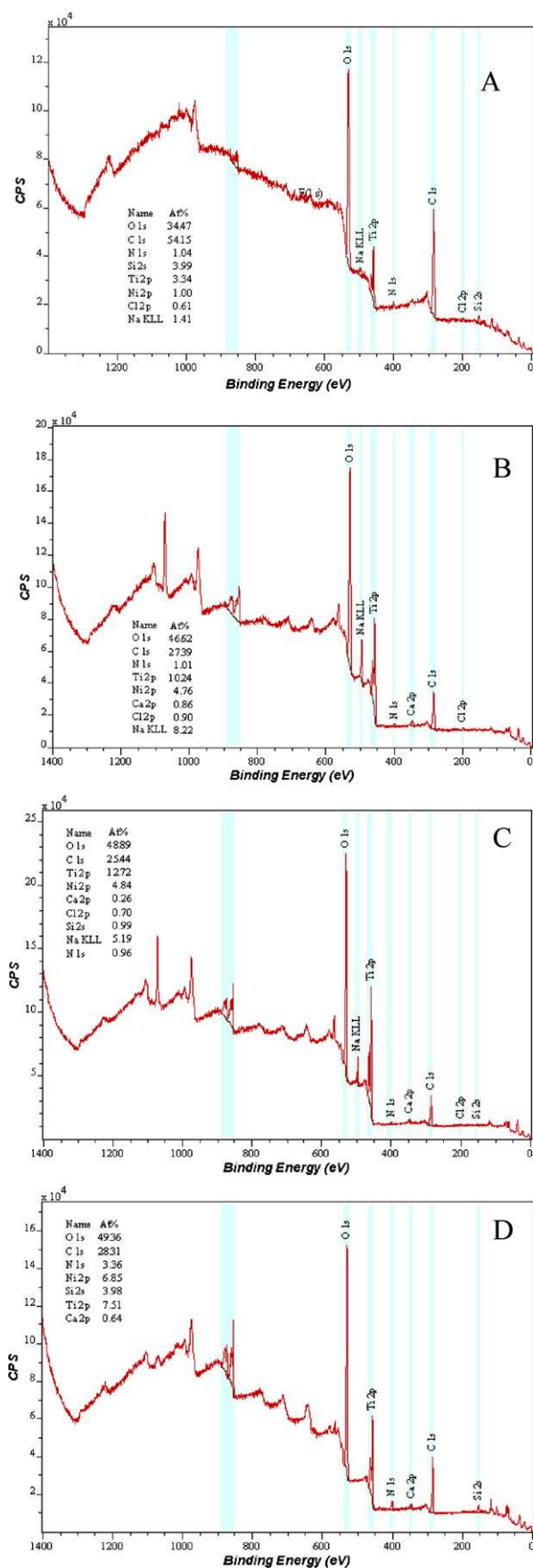


**Fig. 7.** XPS survey spectra of the surface of NiTi: (A) NiTi alloy as received, (B) anodised NiTi, (C) heat treated at 600 °C and (D) silanised NiTi (cps=counts per second).

**Table 2**

Composition of the Si compositions (in wt.%) measured by EDX for different silane modification scenarios. (A) 2%, 15 min, pH=8; (B) 2%, 15 min, pH=4; (C) 2%, 1 h, pH=8; (D) 2%, 1 h, pH=4; (E) 5%, 1 h, pH=8.

Spectrum	A	B	C	D	E
Sample 1		1.68	1.33		0.48
Sample 2		3.11		0.68	0.31
Sample 3		0.89			0.94
Sample 4	0.44	0.62	0.58	0.53	0.90
Max.	0.44	3.11	1.33	0.68	0.94
Min.	0.00	0.62	0.58	0.53	0.31

showed Si peaks of moderate intensity indicating that a 5% silane solution at pH=8 and 1 h deposition results in a rather uniform silane film.

The chemistry of the NiTi surface after each step of surface treatment has been studied by XPS. In contrast to EDX, XPS has much higher surface sensitivity (probing depth in the nm rather than mm range). Fig. 7 shows typical XPS survey spectra of the surfaces of the NiTi strip. The analysis of all observed peak intensities in the survey XP spectra allows a quantification of the elemental composition of the surface region probed by XPS. The surfaces of four samples were analyzed: NiTi alloy as received, NiTi after anodisation, NiTi after heat treatment at 600 °C and NiTi after silanisation. Relative atom concentrations (at.%) of all elements found are summarized in Table 3.

As received sample showed a surface dominated by a relatively thick layer of carbon and oxygen. There is a clear preference for a 'capping' layer of TiO<sub>2</sub>. Nickel was detected in low levels, due to attenuation by the carbon/oxygen/titanium over layers. Analysis of the C(1s) and O(1s) high resolution scans suggests a large degree of hydrocarbon contamination on the surface together with carbide. Survey scan reveals surface also consists of N, Na, Cl, Ca and Si. The Si content on the surface is due to the lubricant; which disappears after cleaning and anodisation. The presence of C may be attributed to surface contamination by carbon-containing molecules absorbed from the environment.

The dominant elements after anodisation process are O, C, Ti. The anodised sample showed a surface more enriched in Ti compared to the NiTi as received. Ni content has also increased but not as much as Ti. Titanium again is in a TiO<sub>2</sub> like form, but exhibits broadening to low binding energy, possibly due to a lower oxidation state of titanium (e.g. Ti(III)). Other elements present on the surface are: N, Ca, Cl and Na. The Na content is much higher than in the NiTi as received. This might be because the anodisation has been done in sodium nitrate solution in methanol. Si is not detected in the sample after cleaning and anodisation.

Heat treated sample again shows preference for Ti (as TiO<sub>2</sub>) at the surface. C, N, Na, Ca, Cl and Si are also present. Ni is present as Ni(II), shape of spectra is characteristic of NiO. It is worth noting that the heat treatment process has affected the Ti content more than Ni. The surface Ti concentration of the heat treated sample can be as high as 12.72 at.%. These results suggest that the anodised sample is covered by a titanium oxide film. The silanised sample shows preference for Ti (as TiO<sub>2</sub>) at the surface. No sodium was detected. N(1s) intensity has increased. High resolution scans of N(1s) level reveals two nitrogen states, 399.4 and 401.2 eV. The former may be characteristic of NH<sub>x</sub> like species, whereas the latter is more than likely associated with a surface bond. This is because of the NH<sub>2</sub> group in 3-aminopropyltriethoxysilane used in the silanisation process. Detection of the Si signal also indicates silanisation has occurred.



**Table 3**

Surface composition obtained from the quantification of the XPS survey spectra.

Element	NiTi alloy (as received)		Anodised NiTi		Heated treated NiTi at 600 °C		Silanised NiTi	
	At.%	BE	At.%	BE	At.%	BE	At.%	BE
O 1s	34.47	530.41	46.62	530.03	48.89	530.01	49.36	530.034
C 1s	54.15	284.912	27.39	285.03	25.44	285.51	28.31	285.34
N 1s	1.04	399.91	1.01	398.53	0.96	399.51	3.36	400.34
Si 2s	3.99	152.91					3.98	153.84
Ti 2p	3.34	458.41	10.24	458.03	12.72	458.51	7.51	458.34
Ni 2p	1.00	855.41	4.76	855.53	4.84	855.01	6.85	855.34
Ca 2p			0.86	384.03	0.26	347.01	0.64	346.84
Na KLL	1.41	495.41	8.22	495.53	5.19	496.51		

### 3.3. Bond strength

The cross section of the polymer coatings deposited by EHDA and casting on modified NiTi is compared in Fig. 8. Cast coatings (Fig. 8A) are more irregular compared with the electrospayed coatings

(Fig. 8B and C). In addition, in the case of electrospayed coatings the thickness can be varied very effectively by adjusting spraying time. Peel strength data (Fig. 9) confirm that a significant improvement in adhesion can be achieved by using the described modification procedures. Analysis of the data shows that above an extension of

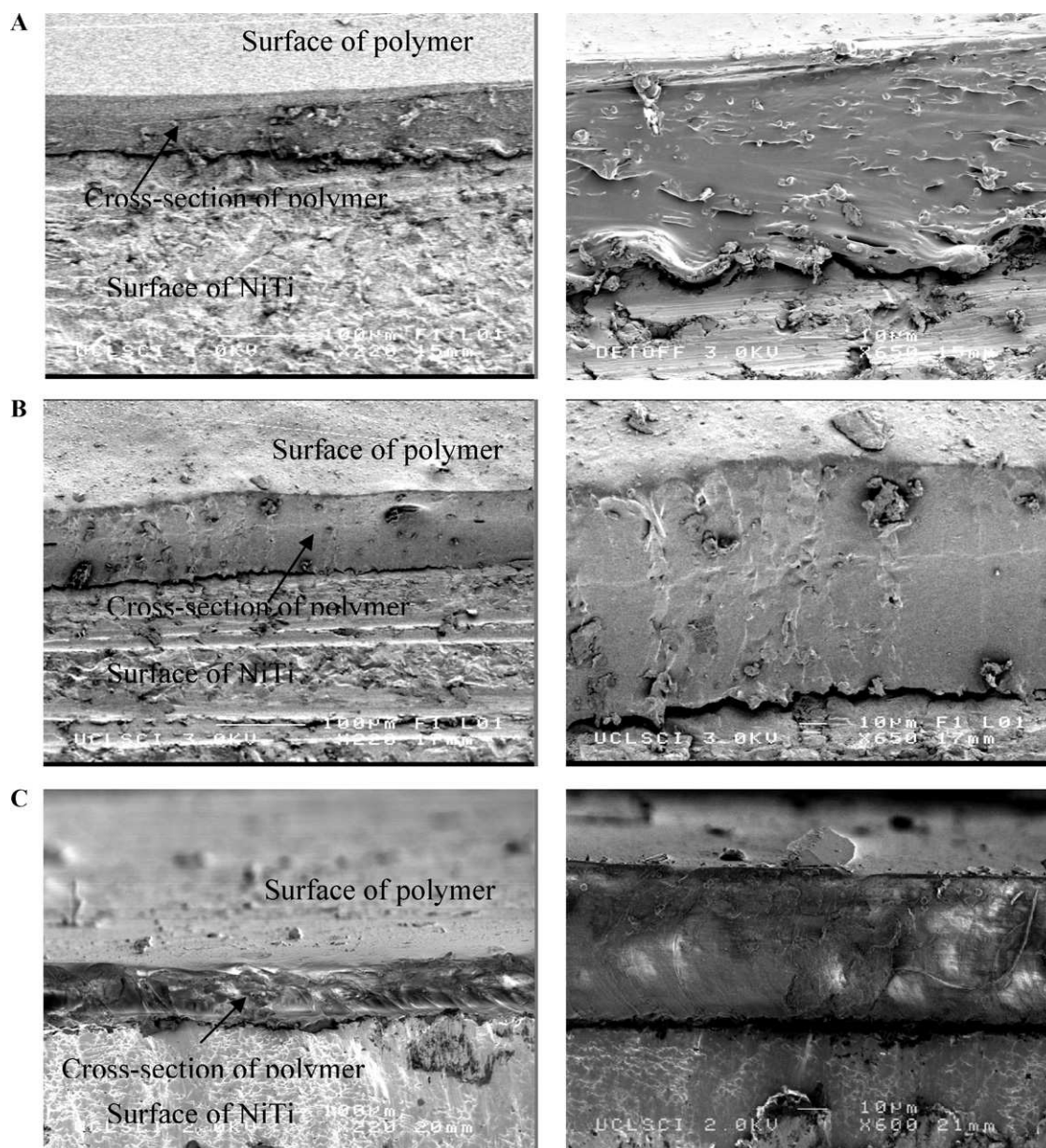


**Fig. 8.** Scanning electron micrographs showing cross-sections of treated, coated NiTi strip: (A) cast coating (B) electrospayed, 100 μm thick polymer coating; (C) electrospayed, 50 μm thick polymer coating.



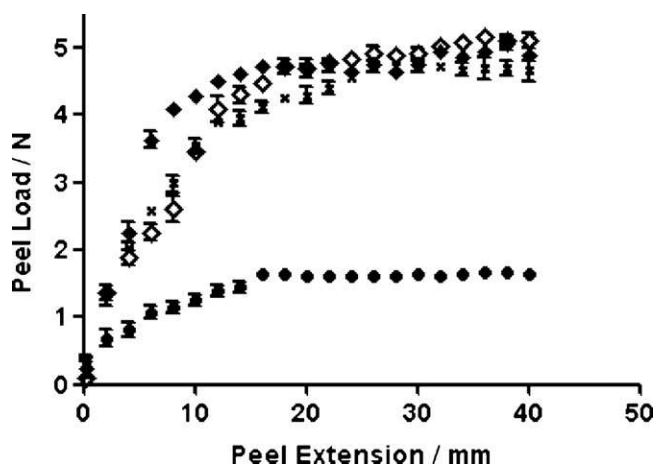


Fig. 9. Peel strength test results for untreated and treated NiTi strip. (◇) 100  $\mu\text{m}$  electro sprayed coating on treated NiTi; (◆) 50  $\mu\text{m}$  electro sprayed coating on treated NiTi; (■) cast coating on treated NiTi; (●) untreated NiTi.

25 mm the load required to remove the polymer from the modified strip for all the samples is on average three times greater than that for the control.

There is no significant difference between the bonding strength as a result of the different coating methods. Considering EHDA deposition, the peel strength of the 100  $\mu\text{m}$  thick polymer coating is slightly greater than the 50  $\mu\text{m}$  thick coating. It should be noted that below an extension of 10 mm, all the curves of the modified specimens show a positive slope. In this range the applied load is not high enough to break the bond between the polymer and the strip; however, the applied extension causes the exposed polymer (i.e. the polymer that was manually peeled from the strip) to strain. The initial region of the curve should be ignored and it is not significant to the overall peel strength measured. It is possible to apply a coating thickness of <10  $\mu\text{m}$ , however such specimens are difficult for peel strength testing. So, the specimen thickness used in this study was increased to facilitate peel strength testing. The proposed surface treatment can be applied to a range of strut/wire thickness. Yin et al. [47] used the same peel test technique for assessment of bonding strength of the coating on metal surfaces.

### 3.4. Coating stability

The morphological changes and the integrity of the coating in the course of the degradation are of great interest to researchers who are developing the new stents [48,49]. Fragmentation or delamination of thin coating from the strut surface during degradation process may present safety concerns. The stability of the PLGA coating upon hydrolysis degradation has been investigated by other researcher [48]. In this study, we have considered other factors such as enzymes and free radicals, which may also influence the degradation. The surface topography of the aged samples is shown in Fig. 10. Topographic and structural changes due to aging can influence the adhesion properties of the coating, leading to coating failures. The polymer coating incubated in distilled water characteristically showed a smooth and uniform surface (Fig. 10A). No cracks or failure of the coatings were also observed for the polymer coating subjected to hydrolysis (Fig. 10B and C). The coating exposed to plasma fractions still appears uniform, which indicates sufficient interfacial adhesion (Fig. 10D and E). Pores or surface cracking is visible on the surface of the nanocomposite exposed to oxidative degradation (Fig. 10F). Therefore, the nanocomposite coating incubated in  $\text{H}_2\text{O}_2$  solution does not exhibit the required resistance to oxidative environment. This effect was even more pronounced with the *t*-butyl peroxidation systems (Fig. 10G).

In this study, peel strength analysis showed that, in spite of accelerated degradation, the coating showed no significant difference in adhesion properties between the control, hydrolytic and plasma-degraded nanocomposites (Fig. 11). This is an indicator of the stability of the surface modification applied and coating durability to these types of *in vitro* degradation. When compared to the similar experiments performed on non-modified NiTi, the modified NiTi showed significantly greater stability in a degradative environment. In fact, the non-modified specimens lost their polymer coating completely after a few weeks. The surface modification proposed retained its effectiveness to promote coating adhesion to the NiTi. It is important to note, however, that in the case of  $\text{H}_2\text{O}_2$  and *t*-butyl-peroxide-degraded nanocomposites, a decrease in peel strength was observed. The  $\text{H}_2\text{O}_2$  (Co) solution provides an oxidative reaction comparable to that observed in the functional activity of the inflammatory cells in response to some biomaterials [50]. However, we used a solution concentration of 1.63 M  $\text{H}_2\text{O}_2$ , which is very high compared to that reported by Lee et al. [51]; which is <20  $\mu\text{mol}$ . Therefore, except in aggressive oxidative environments, the polymer coating on the modified NiTi stent alloy withstands effects of biological environments. The coating maintained its integrity and strong adhesion to the strut during the entire degradation process without any signs of instability or delamination. The problem of delamination requires full consideration of the interface between the coating and the underlying substrate. Ruptures and cracks could be problematic by inducing fast restenosis and uneven surface structures are a major cause of thrombogenic events with stent implants [52]. Therefore, coatings are expected to minimize the risk of bare metal parts getting into direct contact with tissue throughout the stent lifetime.

It is also interesting to note that the internal residual stress or applied external stress may also have effects on the degradation rate [53]. A few studies also investigated the effect of mechanical strain forces encountered during stent deployment. They have examined the integrity of the coating on the stent by studying any sign of cracking or delamination of the coating after balloon expansion and implantation [54–57]. In future work, we evaluate the POSS–PCU as the potential stent coating after accelerated durability testing and upon stent expansion to the maximal diameter. Accelerated durability test is to evaluate failure modes such as fretting, abrasion, and wear under pulsatile flow and physiologic loading that simulates blood pressure conditions in the artery.

### 3.5. Corrosion resistance

Three sets of NiTi strips were chosen for corrosion resistance studies. The first group is surface modified NiTi strip coated with POSS–PCU according to the method which has been shown to lead to a much greater resistance to decay in peel strength compared to untreated NiTi. The second group is untreated NiTi strip coated with POSS–PCU. The bare NiTi strips have been chosen as the control. The Ni release from all three groups in DMEM was measured by ICP–MS.

The Ni release tests (Fig. 12) clearly show the effect of coating NiTi samples with POSS–PCU, even after one hour. Ni release is much greater from the bare NiTi samples, reaching 1784 ng/mL in DMEM after 3 days compared to 4.16 ng/mL, respectively, for surface treated sprayed NiTi samples ( $p$  value =  $3 \times 10^{-8}$ ;  $p$  value < 0.001 which shows a significant difference). In addition, there is also a difference between untreated POSS–PCU coated NiTi samples and surface treated samples. After 3 h, the amount of Ni released from untreated sprayed samples is higher than the amount released from surface treated samples, 13.77 ng/mL released from untreated NiTi samples in DMEM, respectively, compared with 4.163 from surface treated samples ( $p$  value =  $5 \times 10^{-6}$ ;  $p$  value < 0.001 which shows a significant difference). It is also important to note that the POSS–PCU coated samples (both treated

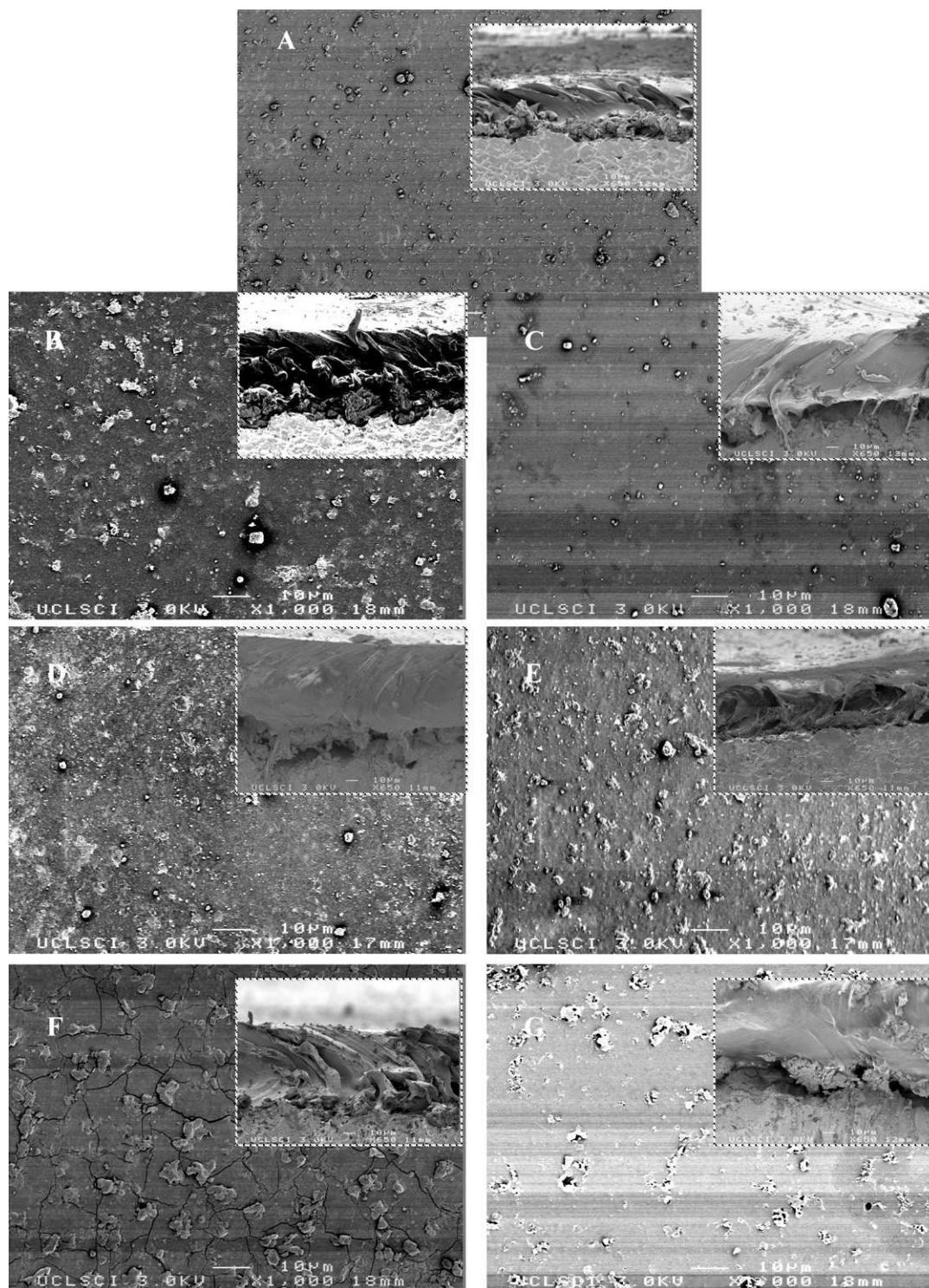


**Fig. 10.** Typical scanning electron micrographs of post-incubated POSS-PCU nanocomposite polymer coating on NiTi in (A) distilled water, (B) cholesterol esterase, (C) phospholipase A2, (D) plasma fraction II, (E) plasma fraction III, (F)  $\text{H}_2\text{O}_2$  and (G) *t*-butyl peroxide after 70 days. Inserts show cross-sections.

and untreated), not only reduce the amount of Ni released, but also significantly reduce the rate at which it is released, shown by the minimal change in Ni concentration between 1 h ( $6.89 \pm 1.97 \text{ ng/mL}$ ) and 72 h ( $13.32 \pm 8.70 \text{ ng/mL}$ ). This is compared to an increase in Ni concentration of more than  $1300 \text{ ng/mL}$  between 1 h and 72 h. Based on these results it is clear that coating with POSS-PCU reduces the amount of Ni released to a negligible amount. Surface treatment process of the NiTi strips before coating helps this effect further. This process increases the strength of the

bond between polymer and NiTi and thereby increases the corrosion resistance. This is of great importance as the release of Ni from NiTi can result in tissue damage and therefore delay healing and increase of the risk of thrombus formation [58,59].

Electrochemical anodisation was also employed in another study to form a layer of  $\text{TiO}_2$  layer on the titanium substrate, to improve the biocompatibility of biomedical implants [60]. Covalent attachment of coating onto the stents surface reduced thrombogenicity of the titanium [61]. In summary, an approach

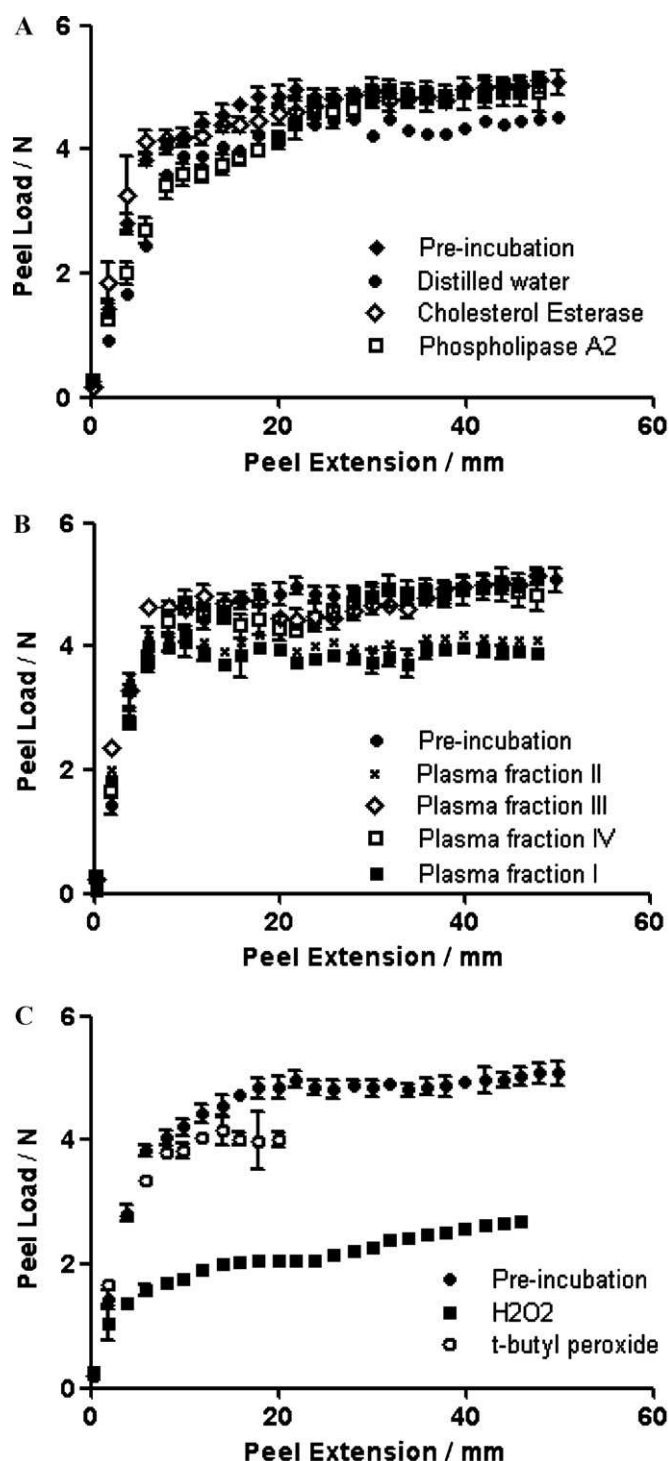


Fig. 11. Peel strength test of coated NiTi strip following 70 days immersion in different media. (A) Hydrolytic solutions, (B) plasma fractions and (C) oxidative/peroxidative solutions.

for depositing the POSS-PCU onto NiTi self-expandable stent is outlined. This involves pre-modification of the metal alloy and electrohydrodynamic polymer deposition. The optimum surface modification protocol has been deduced. The coating has the potential to protect the materials surface, mitigate corrosion and increase the longevity of the device *in vivo*. The results of peel strength have shown that a three fold increase in the bond strength of the POSS-PCU to the metal alloy can be readily achieved upon surface modification. Comparative *in vitro* degradation of the coat-

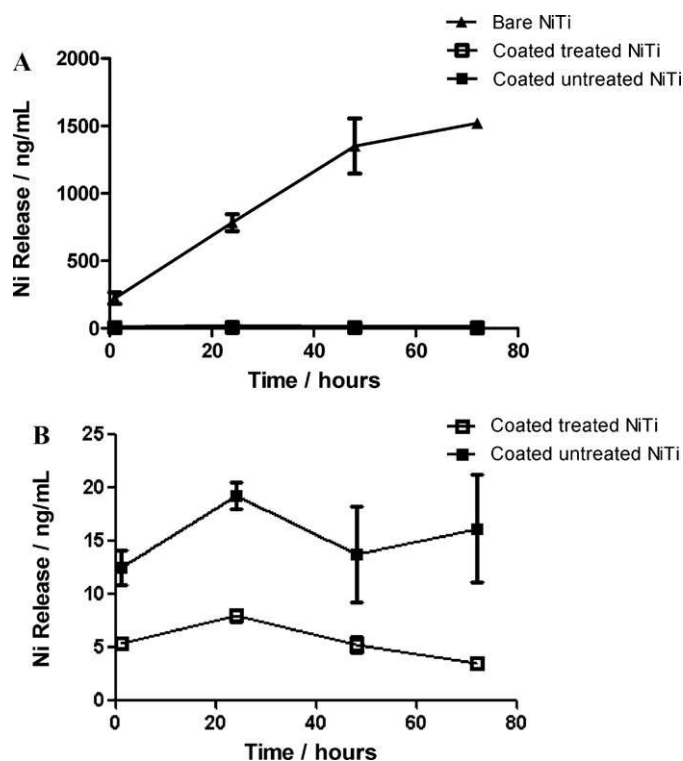


Fig. 12. Ni release profiles from NiTi strips obtained from mass spectroscopy. Strips were incubated in DMEM. Inset: (A) negligible Ni release from coated NiTi compared with bare NiTi; (B) less Ni release from coated treated NiTi compared with coated untreated.

ing on modified and non-modified NiTi has been carried out and demonstrates the ability of the coating to remain integral with the stent upon long time (70 days) exposure to biological environments under static condition. Ni release profiles showed the dramatic effect that POSS-PCU had on the corrosion resistance of NiTi samples. It is clear that coating with POSS-PCU reduces the amount of Ni released to a negligible amount. This effect is exaggerated by surface treatment of NiTi before coating. This process increases the strength of the bond between polymer and NiTi and thereby increases the corrosion resistance.

#### 4. Conclusion

We have developed and extensively characterized a nanocomposite polymer (POSS-PCU). The POSS-PCU has been manufactured as small diameter bypass graft, which is undergoing clinical trials and under-development for percutaneous heart valve. Here we outline an approach for depositing the POSS-PCU onto NiTi self-expandable stent. This involves pre-modification of the metal alloy and electrohydrodynamic polymer deposition. The optimum surface modification protocol has been deduced. The coating has the potential to protect the materials surface, mitigate corrosion and increase the longevity of the device *in vivo*. The results of peel strength have shown that a three fold increase in the bond strength of the POSS-PCU to the metal alloy can be readily achieved upon surface modification. Comparative *in vitro* degradation of the coating on modified and non-modified NiTi has been carried out and demonstrates the ability of the coating to remain integral with the stent upon long time (70 days) exposure to biological environments under static condition. The next stage of our work is implanting the developed stent *in vivo*.



## Acknowledgements

We would like to acknowledge the comments from Professor Mohan Edirisinghe, Dept of Mechanical Engineering at University College London. The authors would like to acknowledge the financial support of Engineering and Physical Sciences Research Council and National Institute for Health Research for development of a stent.

## References

- [1] M. Es-Souni, M. Es-Souni, H. Fischer-Brandies, Assessing the biocompatibility of NiTi shape memory alloys used for medical applications, *Analytical and Bioanalytical Chemistry* 381 (3) (2005) 557–567.
- [2] S.A. Shabalovskaya, Surface, corrosion and biocompatibility aspects of Nitinol as an implant material, *Biomedical Materials and Engineering* 12 (1) (2002) 69–109.
- [3] S.D. Plant, D.M. Grant, L. Leach, Surface modification of NiTi alloy and human platelet activation under static and flow conditions, *Materials Letters* 61 (14–15) (2007) 2864–2867.
- [4] N. Shafiq, S. Malhotra, P. Pandhi, A. Grover, A. Uboweja, A meta-analysis of clinical trials of paclitaxel- and sirolimus-eluting stents in patients with obstructive coronary artery disease, *British Journal of Clinical Pharmacology* 59 (1) (2005) 94–101.
- [5] A.A. Bavry, D.L. Bhatt, Appropriate use of drug-eluting stents: balancing the reduction in restenosis with the concern of late thrombosis, *Lancet* 371 (9630) (2008) 2134–2143.
- [6] V.C. Karakiozaki, S.D. Logothetidis, S.N. Kassavetis, G.D. Giannoglou, Nanomedicine for the reduction of the thrombogenicity of stent coatings, *International Journal of Nanomedicine* 5 (2010) 239–248.
- [7] K. Maekawa, K. Kawamoto, S. Fuke, R. Yoshioka, H. Saito, T. Sato, et al., Severe endothelial dysfunction after sirolimus-eluting stent implantation, *Circulation* 113 (23) (2006) E850–E851.
- [8] M.W.I. Webster, J.A. Ormiston, Drug-eluting stents and late stent thrombosis, *Lancet* 370 (9591) (2007) 914–915.
- [9] M.R. Bennett, In-stent stenosis: pathology and implications for the development of drug eluting stents, *Heart* 89 (2) (2003) 218–224.
- [10] A.V. Finn, F.D. Kolodgie, J. Harnek, L.J. Guerrero, E. Acampado, K. Tefera, et al., Differential response of delayed healing and persistent inflammation at sites of overlapping sirolimus- or paclitaxel-eluting stents, *Circulation* 112 (2) (2005) 270–278.
- [11] M. Kollum, A. Farb, R. Schreiber, K. Terfera, A. Arab, A. Geist, et al., Particle debris from a nanoporous stent coating obscures potential antiproliferative effects of tacrolimus-eluting stents in a porcine model of restenosis, *Catheterization and Cardiovascular Interventions* 64 (1) (2005) 85–90.
- [12] M.M. Mazumder, S. De, S. Trigwell, N. Ali, M.K. Mazumder, J.L. Mehta, Corrosion resistance of polyurethane-coated nitinol cardiovascular stents, *Journal of Biomaterials Science, Polymer Edition* 14 (12) (2003) 1351–1362.
- [13] S. Trigwell, S. De, R. Sharma, M.K. Mazumder, J.L. Mehta, Structural evaluation of radially expandable cardiovascular stents encased in a polyurethane film, *Journal of Biomedical Materials Research Part B: Applied Biomaterials* 76 (2) (2006) 241–250.
- [14] R.J. Zdrachala, Small caliber vascular grafts. Part II. Polyurethanes revisited, *Journal of Biomaterials Applications* 11 (1) (1996) 37–61.
- [15] H.J. Salacinski, N.R. Tai, R.J. Carson, A. Edwards, G. Hamilton, A.M. Seifalian, In vitro stability of a novel compliant poly(carbonate-urea)urethane to oxidative and hydrolytic stress, *Journal of Biomedical Materials Research* 59 (2) (2002) 207–218.
- [16] A.M. Seifalian, H.J. Salacinski, A. Tiwari, A. Edwards, S. Bowald, G. Hamilton, In vivo biostability of a poly(carbonate-urea)urethane graft, *Biomaterials* 24 (14) (2003) 2549–2557.
- [17] R.Y. Kannan, H.J. Salacinski, M. Odlyha, P.E. Butler, A.M. Seifalian, The degradative resistance of polyhedral oligomeric silsesquioxane nanocore integrated polyurethanes: an in vitro study, *Biomaterials* 27 (9) (2006) 1971–1979.
- [18] R.Y. Kannan, H.J. Salacinski, J. De Groot, I. Clatworthy, L. Bozec, M. Horton, et al., The antithrombotic potential of a polyhedral oligomeric silsesquioxane (POSS) nanocomposite, *Biomacromolecules* 7 (1) (2006) 215–223.
- [19] G. Punshon, K.M. Sales, D.S. Vara, G. Hamilton, A.M. Seifalian, Assessment of the potential of progenitor stem cells extracted from human peripheral blood for seeding a novel vascular graft material, *Cell Proliferation* 41 (2) (2008) 321–335.
- [20] M.A. de, G. Punshon, B. Ramesh, S. Sarkar, A. Darbyshire, G. Hamilton, et al., In situ endothelialization potential of a biofunctionalised nanocomposite biomaterial-based small diameter bypass graft, *Biomedical Materials and Engineering* 19 (4–5) (2009) 317–331.
- [21] R.Y. Kannan, H.J. Salacinski, K. Sales, P.E. Butler, A.M. Seifalian, The endothelialization of polyhedral oligomeric silsesquioxane nanocomposites: an in vitro study, *Cell Biochemistry and Biophysics* 45 (2) (2006) 129–136.
- [22] R. Bakhshi, M.J. Edirisinghe, A. Darbyshire, Z. Ahmad, A.M. Seifalian, Electrohydrodynamic jetting behaviour of polyhedral oligomeric silsesquioxane nanocomposite. *Journal of Biomaterials Applications* (2008) [Epub ahead of print].
- [23] A. Gupta, A.M. Seifalian, Z. Ahmad, M.J. Edirisinghe, M.C. Winslet, Novel electrohydrodynamic printing of nanocomposite biopolymer scaffolds, *Journal of Bioactive and Compatible Polymers* 22 (3) (2007) 265–280.
- [24] P. Hale, S. Turgeon, P. Horny, F. Lewis, N. Brack, R.G. Van, et al., X-ray photoelectron emission microscopy and time-of-flight secondary ion mass spectrometry analysis of ultrathin fluoropolymer coatings for stent applications, *Langmuir* 24 (15) (2008) 7897–7905.
- [25] C.G. Hopkins, P.E. McHugh, J.P. McGarry, Computational investigation of the delamination of polymer coatings during stent deployment, *Annals of Biomedical Engineering* 38 (7) (2010) 2263–2273.
- [26] R. Hoffmann, G.S. Mintz, P.K. Haager, T. Bozoglu, E. Grube, M. Gross, et al., Relation of stent design and stent surface material to subsequent in-stent intimal hyperplasia in coronary arteries determined by intravascular ultrasound, *American Journal of Cardiology* 89 (12) (2002) 1360–1364.
- [27] P. Molitor, V. Barron, Y. Young, Surface treatment of titanium for adhesive bonding to polymer composites: a review, *International Journal of Adhesion & Adhesives* 21 (2001) 129–136.
- [28] Food and Drug Administration, Guidance for industry and FDA staff, non-clinical tests and recommended labeling for intravascular stents and associated delivery systems. <http://www.fda.gov/cdrh/ode/guidance/1545.html>, 2005.
- [29] Y. Huang, S.S. Venkatraman, F.Y. Boey, E.M. Lahti, P.R. Umashankar, M. Mohanty, et al., In vitro and in vivo performance of a dual drug-eluting stent (DDES), *Biomaterials* 31 (15) (2010) 4382–4391.
- [30] F. Unger, U. Westedt, R. Wombacher, S. Zimmermann, A. Greiner, et al., Poly(ethylene carbonate): a thermoelastic and biodegradable biomaterial for drug eluting stent coatings? *Journal of Controlled Release* 117 (3) (2007) 312–321.
- [31] Y. Levy, D. Mandler, J. Weinberger, A.J. Domb, Evaluation of drug-eluting stents' coating durability – clinical and regulatory implications, *Journal of Biomedical Materials Research Part B: Applied Biomaterials* 91 (1) (2009) 441–451.
- [32] P. Hanefeld, U. Westedt, R. Wombacher, T. Kissel, A. Schaper, J.H. Wendorff, et al., Coating of poly(p-xylylene) by PLA-PEO-PLA triblock copolymers with excellent polymer–polymer adhesion for stent applications, *Biomacromolecules* 7 (7) (2006) 2086–2090.
- [33] H.J. Kim, M.W. Moon, D.I. Kim, K.R. Lee, K.H. Oh, Observation of the failure mechanism for diamond-like carbon film on stainless steel under tensile loading, *Scripta Materialia* 57 (2007) 1016–1019.
- [34] H. Salacinski, S. Hancock, A.M. Seifalian, inventors, Polymer for use in conduits, medical devices and biomedical surface modification, patent Int. App. PCT/GB2005/000489, 2005, 2005.
- [35] F.T. Cheng, P. Shi, H.C. Man, Nature of oxide layer formed on NiTi by anodic oxidation in methanol, *Materials Letters* 59 (12) (2005) 1516–1520.
- [36] F.D. Blum, W. Meesiri, H.J. Kang, J.E. Gambogi, Hydrolysis, adsorption, and dynamics of silane coupling agents on silica surfaces, *Journal of Adhesion Science and Technology* 5 (6) (1991) 479–496.
- [37] ASTM D413-98(2007) Standard test methods for rubber property-adhesion to flexible substrate, 2009.
- [38] A. Michiardi, C. Aparicio, J.A. Planell, F.J. Gil, New oxidation treatment of NiTi shape memory alloys to obtain Ni-free surfaces and to improve biocompatibility, *Journal of Biomedical Materials Research Part B-Applied Biomaterials* 77B (2) (2006) 249–256.
- [39] S. Shabalovskaya, J. Anderegg, H.J. Van, Critical overview of Nitinol surfaces and their modifications for medical applications, *Acta Biomaterialia* 4 (3) (2008) 447–467.
- [40] W.J. van Ooij, D. Zhu, V. Palanivel, J.A. Lamar, M. Stacy, Overview: the potential of silanes for chromate replacement in metal finishing industries, *Silicon Chemistry* 3 (2006) 11–30.
- [41] Methods for producing adhesive bonds between substrate and polymer employing an intermediate oxide layer, inventors patent *United States Patent* 4364731, 1982, 1982.
- [42] E.M. Petrie, Adhesion & bonding: silanes as primers and adhesion promoters for metal substrates, *Metal finishing* 105 (7–8) (2007) 85–93.
- [43] G.P. Sundararajan, W.J. van Ooij, Silane based pretreatments for automotive steels, *Surface Engineering* 16 (4) (2000) 315–320.
- [44] T. Hu, C.L. Chu, L.H. Yin, Y.P. Pu, Y.S. Dong, C. Guo, et al., In vitro biocompatibility of titanium–nickel alloy with titanium oxide film by H<sub>2</sub>O<sub>2</sub> oxidation, *Transactions of Nonferrous Metals Society of China* 17 (3) (2007) 553–557.
- [45] M. Pohl, T. Glogowski, S. Kuhn, C. Hensing, F. Unterumberger, Formation of titanium oxide coatings on NiTi shape memory alloys by selective oxidation, *Materials Science and Engineering A-Structural Materials Properties Microstructure and Processing* 481 (2008) 123–126.
- [46] S.Z. El Abedin, U. Welz-Biermann, F. Endres, A study on the electrodeposition of tantalum on NiTi alloy in an ionic liquid and corrosion behaviour of the coated alloy, *Electrochemistry Communications* 7 (9) (2005) 941–946.
- [47] A. Wisbey, P.J. Gregson, L.M. Peter, M. Tuke, Effect of surface-treatment on the dissolution of titanium-based implant materials, *Biomaterials* 12 (5) (1991) 470–473.
- [48] X.P. Liu, Y.N. Wang, D.Z. Yang, M. Qi, The effect of ageing treatment on shape-setting and superelasticity of a nitinol stent, *Materials Characterization* 59 (4) (2008) 402–406.
- [49] Y. Yin, S.G. Wise, N.J. Nosworthy, A. Waterhouse, D.V. Bax, Covalent immobilisation of tropoelastin on a plasma deposited interface for enhancement of endothelialisation on metal surfaces, *Biomaterials* 30 (2009) 1675–1681.
- [50] T. Xi, R. Gao, B. Xu, L. Chen, T. Luo, J. Liu, et al., In vitro and in vivo changes to PLA/sirolimus coating on drug eluting stents, *Biomaterials* 31 (19) (2010) 5151–5158.

- [49] Y. Shaulov, R. Okner, Y. Levi, N. Tal, V. Gutkin, D. Mandler, et al., Poly(methyl methacrylate) grafting onto stainless steel surfaces: application to drug-eluting stents, *ACS Applied Materials & Interfaces* 1 (11) (2009) 2519–2528.
- [50] K.A. Hooper, Characterization of the inflammatory response to biomaterials using a rodent air pouch model, *Journal of Biomedical Materials Research* 50 (3) (2000) 365–374.
- [51] D. Lee, In vivo imaging of hydrogen peroxide with chemiluminescent nanoparticles, *Nature Materials* 6 (2007) 765–769.
- [52] F. Unger, U. Westedt, P. Hanefeld, R. Wombacher, S. Zimmermann, A. Greiner, et al., Poly(ethylene carbonate): a thermoelastic and biodegradable biomaterial for drug eluting stent coatings? *Journal of Controlled Release* 117 (3) (2007) 312–321.
- [53] Y.Z. Wan, Y.L. Wang, L.Y. Zheng, F.G. Zhou, Q. Zhao, G.X. Cheng, Influence of external stress on the in vitro degradation behavior of C3D/PLA composites, *Journal of Materials Science Letters* 20 (2001) 1659–1957.
- [54] H.H. Cho, D.W. Han, K. Matsumura, S. Tsutsumi, S.H. Hyon, The behavior of vascular smooth muscle cells and platelets onto epigallocatechin gallate-releasing poly(L-lactide-co-epsilon-caprolactone) as stent-coating materials, *Biomaterials* 29 (7) (2008) 884–893.
- [55] P. Hanefeld, U. Westedt, R. Wombacher, T. Kissel, A. Schaper, J.H. Wendorff, et al., Coating of poly(p-xylylene) by PLA-PEO-PLA triblock copolymers with excellent polymer-polymer adhesion for stent applications, *Biomacromolecules* 7 (7) (2006) 2086–2090.
- [56] X. Wang, X. Zhang, J. Castellot, I. Herman, M. Iafrati, D.L. Kaplan, Controlled release from multilayer silk biomaterial coatings to modulate vascular cell responses, *Biomaterials* 29 (7) (2008) 894–903.
- [57] U. Westedt, M. Wittmar, M. Hellwig, P. Hanefeld, A. Greiner, A.K. Schaper, et al., Paclitaxel releasing films consisting of poly(vinyl alcohol)-graft-poly(lactide-co-glycolide) and their potential as biodegradable stent coatings, *Journal of Controlled Release* 111 (1–2) (2006) 235–246.
- [58] C. Heintz, G. Riepe, L. Birken, E. Kaiser, N. Chakfe, M. Morlock, et al., Corroded nitinol wires in explanted aortic endografts: an important mechanism of failure? *Journal of Endovascular Surgery* 8 (3) (2001) 248–253.
- [59] M. Berger-Gorbet, B. Broxup, C. Rivard, L.H. Yahia, Biocompatibility testing of NiTi screws using immunohistochemistry on sections containing metallic implants, *Journal of Biomedical Materials Research* 32 (2) (1996) 243–248.
- [60] Y. Yang, Q. Zhang, K. Wu, L. Zhang, C. Lin, P. Tang, A novel electrochemical strategy for improving blood compatibility of titanium-based biomaterials, *Colloids and Surfaces. B, Biointerfaces* 79 (1) (2010) 309–313.
- [61] S. Ye, C.A. Johnson Jr., J.R. Woolley, H. Murata, L.J. Gamble, K. Ishihara, et al., Simple surface modification of a titanium alloy with silanated zwitterionic phosphorylcholine or sulfobetaine modifiers to reduce thrombogenicity, *Colloids and Surfaces. B, Biointerfaces* 79 (2) (2010) 357–364.